

# Effect of impact-parameter-dependent electronic energy loss on reflected-ion spectra



V.I. Shulga<sup>a</sup>, A. Schinner<sup>b</sup>, Peter Sigmund<sup>c,\*</sup>

<sup>a</sup> Skobeltsin Institute of Nuclear Physics, Lomonosov Moscow State University, 119992 Moscow, Russia

<sup>b</sup> Department of Experimental Physics, Johannes Kepler University, A-4040 Linz, Austria

<sup>c</sup> Department of Physics, Chemistry and Pharmacy, University of Southern Denmark, DK-5230 Odense M, Denmark

## ARTICLE INFO

### Keywords:

Ion beam  
Backscattering  
Energy spectra  
Electronic stopping  
Impact parameter dependence

## ABSTRACT

Conventional theory and computation of the slowing-down of ions and associated radiation effects relies on a scheme proposed by Lindhard and Scharff, in which electronic energy losses enter as a friction force. We study limitations of this scheme, when the dependence of electronic losses on the impact parameter in individual atomic collisions is taken into account. We study this feature on the projected range – where it is found to be insignificant – and on reflected-ion spectra – where major changes are observed, dependent on ion energy and ion-target combination. Most sensitive are the position of the peak in the reflected-energy spectrum as well as the behavior near the maximum energy loss. Systems studied include He-Ag, Ne-Ag, B-Si and D-Pt.

## 1. Introduction

Accepted theory and simulation codes of ion penetration and ion-beam-induced radiation effects rely on a scheme introduced by Lindhard et al. (LSS) more than fifty years ago [1]. In this model, interactions are classified into nuclear collisions obeying the laws of classical elastic scattering, whereas electronic energy loss enters as a continuous friction force. This model has been very successful in both fundamental and applied ion beam physics.

Electronic energy transfer in atomic collisions depends on the scattering angle via the impact parameter. This feature is ignored in the LSS description, based on the fact that:

- angular deflection of an ion colliding with electrons is negligible compared to deflection due to interaction with a nucleus, and
- nuclear energy losses, while dominating in central encounters, decrease rapidly with increasing impact parameter, in contrast to electronic interactions which may range considerably beyond atomic dimensions.

While the LSS model has been developed originally to describe ion ranges [1] and radiation damage [2], it has been utilized also in situations where one may question its validity. An example is the well-known standard technique to measure ionic stopping cross sections, where the energy spectrum is measured after transmission through a thin foil. By restricting measurement to a narrow cone around the

direction of incidence of the beam, energy loss to nuclear collisions is greatly reduced, so that electronic energy loss may become dominating [3,4]. However, electronic energy loss depends on the impact parameter and, by and large, increases with the scattering angle. Therefore, electronic stopping may be underestimated, if the analysis is based on the LSS scheme [5].

An early attempt to measure angular dependence of electronic energy loss in solids was reported in Ref. [6] for 7 MeV protons penetrating metallic foils. Later on, measurements with ions like Ne at velocities close to the Bohr speed  $v_0$  were reported in Ref. [7]. In theoretical studies we found a significant influence of the impact-parameter dependence of energy loss, called ‘ $p$ -dependence’ in the following, on extracted electronic stopping cross sections measured by the transmission technique [5,8].

While one may expect that all those aspects of particle penetration and radiation effects that involve electronic stopping to some extent are influenced by  $p$ -dependence, this influence must vary dependent on the considered phenomenon and experimental geometry. We shall see below that the mean projected range is only marginally affected. On the other hand,  $p$ -dependence determines electronic straggling, which is ignored in the LSS scheme. Therefore, straggling deserves separate study. Reflected ions may be viewed as a tail in the backward distribution of the depth profile, and hence a sensitive indicator of straggling.

Analysis of the reflected current has been proposed [9] to experimentally determine electronic stopping cross sections and has since

\* Corresponding author.

<https://doi.org/10.1016/j.nimb.2020.01.029>

Received 30 November 2019; Received in revised form 29 January 2020; Accepted 30 January 2020

Available online 15 February 2020

0168-583X/ © 2020 Elsevier B.V. All rights reserved.

been applied in numerous studies, mainly with low-velocity proton beams. Measurements by the reflection technique serve as indicators for subtle effects like threshold behavior of electronic stopping. This warrants an analysis of the procedure leading from a measured energy or time-of-flight spectrum to a stopping cross section.

There is a large body of studies on ion reflection, both theoretical and simulational [10] as well as experimental. In many cases the quantity aimed at has been the total reflection coefficient for particles and for energy. Also joint distributions of energy and angle of reflected ions have been found, mostly by Monte Carlo simulation. Amongst those, the MARLOWE code [11] stands out, because it allows incorporation of  $p$ -dependence [12]. The model for  $p$ -dependence was based on a modification of Firsov's formula [13], but an estimate of the difference between allowing and excluding  $p$ -dependence was not reported.

Here we report reflected-ion spectra simulated by the OKSANA code [14] allowing for  $p$ -dependence primarily on the basis of the PASS code [15,16] and the Firsov formula [13,17], in analogy to the approach taken in [5]. In a subsequent paper the scheme will be applied to the extraction of stopping cross sections in the reflection mode.

## 2. Input

### 2.1. Impact-parameter-dependent energy loss

The primary quantity of interest in the present context is the function  $T_e(E, p)$  expressing the mean electronic energy loss  $T_e$  of an ion with an initial energy  $E$  in a collision with an atom at impact parameter  $p$ , from which the stopping cross section  $S_e(E)$  can be determined as a function of energy via the relation

$$S_e(E) = \int_0^\infty 2\pi p dp T_e(p). \quad (1)$$

Binary stopping theory [15] is based on Bohr's theory [18], which operates with a classical target electron initially at rest. A more realistic model requires several extensions, which have been described in the literature, most recently in [19]. In the present context, the most important extension is the shell correction, which accounts for the statistical distribution of target electrons in real and velocity space.

Since the stopping cross section represents an integral over the spatial distribution, only the velocity distribution enters  $S_e(E)$  via a kinematic transformation, while the spatial dependence does not occur explicitly [20]. This results in stopping cross sections tabulated in Refs. [21,19].

Conversely, the shell correction for  $T_e(E, p)$  is more complex than the one for  $S_e(E)$ . The impact parameter entering Bohr theory refers to the ion–electron interaction, while  $p$  in  $T_e(E, p)$  denotes the ion–nucleus interaction. This involves the spatial distribution of the target electrons around the nucleus and, hence, a 6-fold instead of a 3-fold integration which is a computational challenge [16]. Several numerical tools have been explored in Ref. [16], and results were compared with those from other theoretical models [22,23] as well as experimental data.

In the present context, the prime criterion for validity of the  $T_e(E, p)$  function is that Eq. (1) be obeyed. A systematic check revealed that by far the most accurate agreement between  $S_e(E)$  found directly and by Eq. (1), respectively, is found in what we called option T1 in Ref. [16]. This happens to be the computationally least complex option as well as the one exclusively applied in our recent work [5,8].

An example is shown in Fig. 1, which shows PASS output  $T_e(E, p)$  for H in Ag. Only 9 subshells have been included for Ag, while the 5s shell containing free electrons needs to be treated separately.

Fig. 2 shows a difference of up to 10% between stopping cross sections calculated by PASS directly and via integration of  $T_e(E, p)$ , respectively. While a discrepancy of 10% is common in theoretical predictions of stopping cross sections in the covered energy range, it is too large in the present context. Therefore, in all comparisons, values of

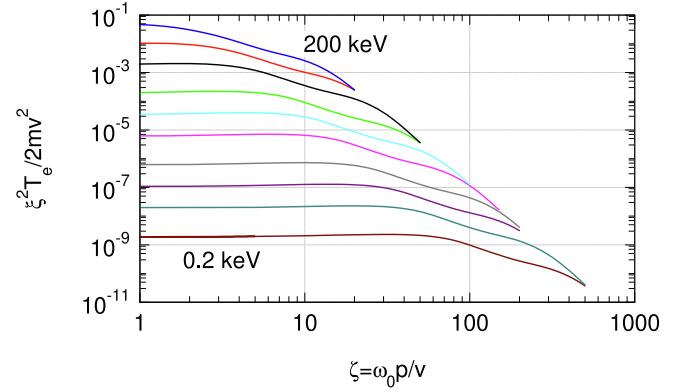


Fig. 1. Mean energy loss  $T(E, p)$  for H in Ag versus impact parameter  $p$  in dimensionless units, where  $\xi = mv^3/Z_1 e^2 \omega$  and  $\zeta = \omega p/v$ ,  $\omega = I/\hbar$  and  $I$  the mean excitation energy or  $I$ -value. Energies 200, 100, 50 etc. keV down to 200 eV, top to bottom. 5s shell not included.

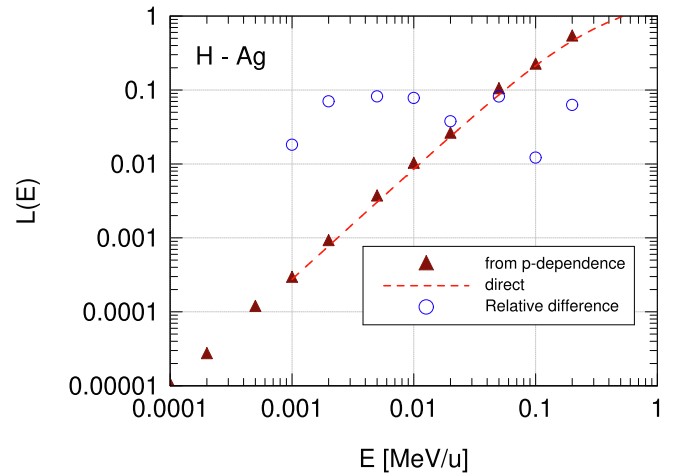


Fig. 2. Stopping number  $L(E) = (mv^2/(4\pi Z_1^2 n_e e^4)) S_e(E)$  for H-Ag, where  $n_e = 46$  is the number of electrons on the target atom. See text.

$S_e$  are the ones determined by integration of  $T_e(E, p)$ .

### 2.2. Simulation code and transport theory

Simulations were performed with the OKSANA code [24,14], which is basically a binary-collision code operating on a crystal lattice with a correction for three-body collisions at low energies. Like in MARLOWE [11], a polycrystalline or amorphous target is simulated by rotating the crystal randomly after every collision.

In the present work, either a Molière potential with Lindhard screening radius has been applied, or the ZBL potential [25]. Electronic energy losses were treated either by the Firsov formula [13] or by PASS output as in case of transport theory.

In the following we distinguish between results denoted  $T(p)$  based on impact-parameter-dependent electronic stopping, and  $S_e$  based on electronic stopping treated as a friction force.

As a preliminary exercise we have looked at ion ranges. According to [1] the mean projected range  $R_p(E)$  is determined from a transport equation which can be written in the form

$$N \int d^2p [R_p(E) - \cos\phi R_p(E - T_n(p) - T_e(p))] = 1, \quad (2)$$

where  $N$  denotes the number of atoms per volume,  $T_n$ ,  $T_e$  nuclear and electronic energy loss, and  $\phi = \phi(E, T_n(p))$  the scattering angle, which is assumed to be solely determined by elastic scattering.

In the LSS approximation, any coupling between electronic and

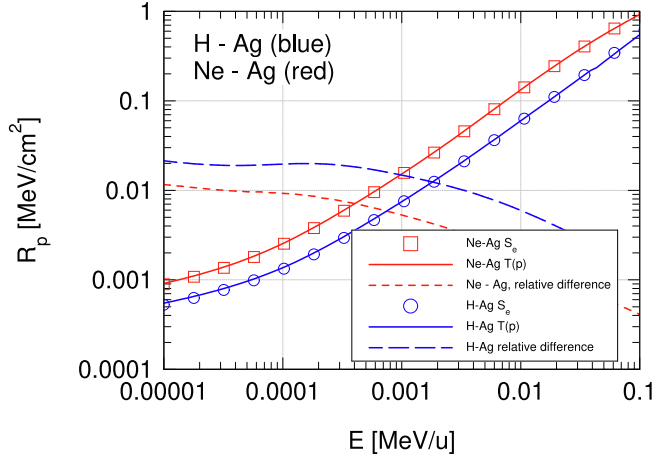


**Fig. 3.** Projected range versus energy, calculated with  $p$ -dependence (solid lines), with friction-like stopping (points), and the relative difference (broken lines), for H-Ag (blue circles) and Ne-Ag (red squares). (For interpretation of the references to colour in this figure legend, the reader is referred to the web version of this article.)

nuclear collisions is ignored. Furthermore, angular deflection in electronic collisions is negligible for heavy ions, and  $T_e(p)$  is considered small so that (2) reduces to

$$N \int d^2p [R_p(E) - \cos\phi R_p(E - T_n)] = 1 - NS_e(E) \frac{dR_p(E)}{dE}. \quad (3)$$

Eqs. (2) and (3) have been evaluated numerically assuming a Molière potential with the Lindhard screening radius and PASS output for  $T_e(E, p)$ . The stopping cross section  $S_e(E)$  entering (3) was determined from (1). Fig. 3 shows a comparison of mean projected ranges computed in the two modes for H-Ag and Ne-Ag. The difference is invisible on the graph, but the broken lines indicate that it decreases with energy and does nowhere exceed 2 pct. These results were fully confirmed by simulation with the OKSANA code (not shown).

### 3. Reflected-ion spectra

As mentioned previously, this work has been stimulated by the reflection technique used in the experimental determination of electronic stopping cross sections [9], in particular at low beam energies down to below 1 keV/u. Special interest has been on the H-Ag system [26].

However, PASS has been developed – and found most reliable – for ions heavier than helium. Therefore we first explore the situation for a couple of heavier ions.

In the following we multiply  $S_e(E)$  and  $T_e(E, p)$  by a factor  $A$  which may differ from  $A = 1$ . In addition to toggling on and off electronic energy loss, variation of  $A$  allows to test the sensitivity of the reflection spectrum to the adopted expression for electronic stopping.

#### 3.1. Ne-Ag

For preliminary orientation we have made two runs on the Ne-Ag system at two widely different beam energies, 100 and 2 keV, respectively (Fig. 4). The main purpose with this is to demonstrate the similarity of the 100 keV spectrum with what is known from Rutherford scattering with more or less well-defined edges determined by the thickness of the sample, and the low-energy spectrum, where the plateau has degenerated into a sharp peak. Computations were based on Firsov's expression for electronic stopping [13]. For 2 keV,  $T(p)$  curves have been computed with both Molière or ZBL interaction potentials. It is seen that for this system, spectra are more sensitive to the elastic-scattering potential than to the handling of electronic energy loss, i.e.,  $T(p)$  or  $S_e$  mode.

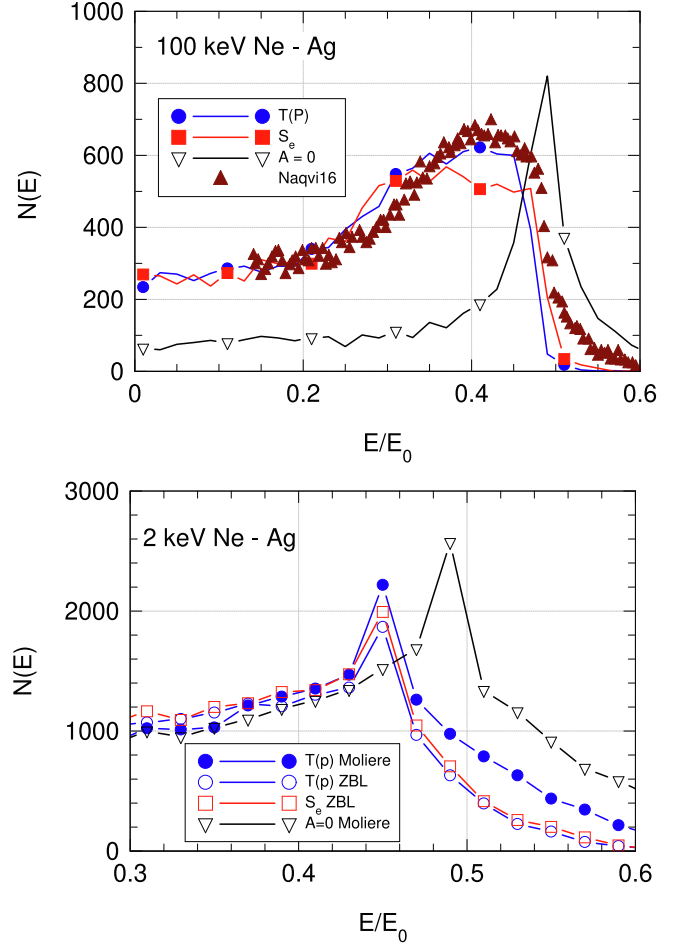


**Fig. 4.** Energy spectra of reflected ions for Ne incident on Ag. ZBL interaction potential,  $T_e(p)$  according to Firsov [13],  $A = 0$  denotes neglect of electronic energy loss. Experimental data from [27]. 1,000,000 runs. Top: 100 keV; bottom: 2 keV.

We note that the peak position for  $A = 0$  is at  $E/E_0 \sim 0.49$  in both graphs. This is below the maximum energy at  $E/E_0 \sim 0.6$ . This shift is determined by elastic-scattering dynamics in conjunction with the energy loss.

For 100 keV beam energy experimental data from Ref. [27] have been included. Since experimental data are given in arbitrary units, a comparison between calculations and measurements must address the shape of the curves rather than the absolute magnitude.

#### 3.2. B-Si

Fig. 5 shows reflected-ion spectra generated by PASS and OKSANA for B-Si at four different beam energies  $E_0$ . In addition to data found by  $T(p)$  (filled blue circles) and  $S_e$  (filled red squares), data have also been included where electronic energy loss has been ignored (empty black triangles,  $A = 0$ ).

As expected, ignoring electronic stopping altogether causes drastic changes in the spectrum at the highest beam energy,  $E_0 = 10$  keV. This difference decreases as  $E_0$  decreases and nuclear stopping increases in importance. Conversely, the difference between the  $S_e$  and  $T(p)$  spectra has the opposite trend. It is barely visible at 10 and 5 keV, but at 1 keV and even more at 0.5 keV we see a clear difference in the peak positions as well as in the tails to the right of the peak.

The large variation in the peak positions at low  $E_0$  is clearly related to the electronic energy loss in low- $p$  collisions. Note that this variation is only found in the  $T(p)$  data, whereas the peak position of the  $S_e$  data

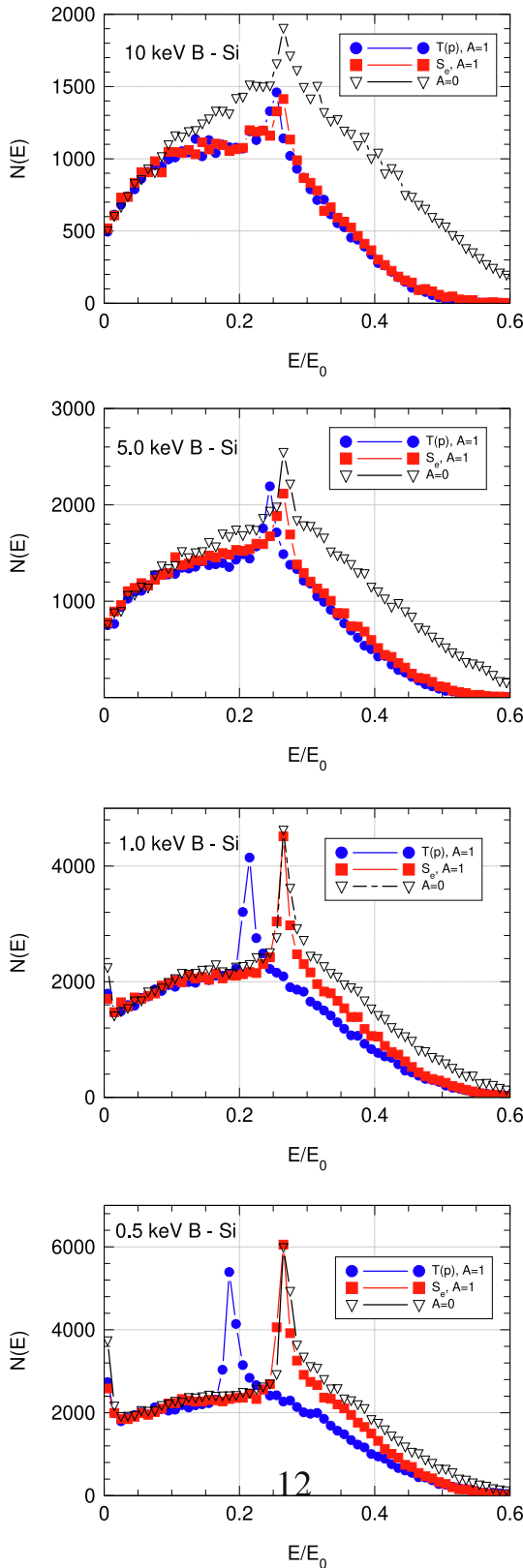


**Fig. 5.** Calculated energy spectra for B-Si, normal incidence, scattering angle  $129^\circ$ , primary energy 10, 5, 1 and 0.5 keV. Electronic stopping from PASS, elastic scattering from Molière potential with Lindhard screening radius, 16 million runs. Multiplication of  $T_e(p)$  by a factor  $A$ , here  $A = 1$  or  $A = 0$ , allows to estimate the sensitivity to the magnitude of electronic stopping. The ordinate  $N(E)$  denotes the number of counts.

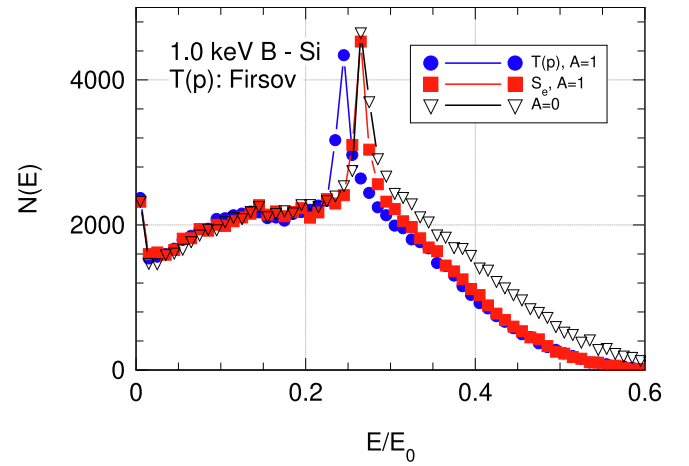


**Fig. 6.** Same as Fig. 5 for  $E = 1$  keV, with electronic energy loss according to Firsov [13] instead of PASS.

is the same as when electronic stopping is altogether neglected.

Since one might suspect this difference to be an artifact of the PASS code, the same situation has been modeled in Fig. 6 for 1 keV but on the basis of the Firsov formula for  $T_e(p, E)$  and  $S_e(E)$  determined from (1). It is seen that in the Firsov case the difference in peak position at 1 keV is only half of that found from PASS. This is a consequence of a more pronounced  $p$ -dependence of the electronic energy loss in PASS, as already experienced in Ref. [5].

Fig. 7 shows analogous spectra at 1 keV for PASS output, but with a factor  $A$  on  $T_e(E, p)$  and, consequently, on  $S_e(E)$ . For clarity  $T(p)$  spectra (top) and  $S_e$  spectra (bottom) have been plotted separately. Spectra have been normalized to the integral over curves for  $A = 1$ . The purpose of this graph is to get an impression of the sensitivity of the spectrum to the electronic stopping cross section.

As to be expected, peak positions depend on  $A$  in the  $T(p)$  data, in contrast to the  $S_e$  data, where the peak position is determined by elastic scattering. Evidently, also the left and right tails depend on  $A$ , the difference from  $A = 1$  being larger for  $A = 2$  than for  $A = 0.5$ . Interestingly, for the  $S_e$  case, the dependence on  $A$  is found to be most pronounced in the right tail. In that regime, a similar variation with  $A$  is also found for the  $T(p)$  case. Conversely, the left tail is significantly more sensitive to  $A$  in the  $T(p)$  than in the  $S_e$  case.

### 3.3. D-Pt

As another preliminary we compare output from the code utilized by Bauer and coworkers [9,26] and OKSANA [14]. Fig. 8 shows calculated spectra for D-Pt evaluated by the two codes within the  $S_e$  scheme and the ZBL potential. This system has been chosen since experimental data are available from Ref. [26]. It is seen that the two curves agree with each other and the experimental data within  $\sim 10\%$  except at the lowest energies ( $E/E_0 < 0.5$ ).

### 3.4. H-Ag

Fig. 9 shows energy spectra for protons backscattered from a 226 Å silver layer on a silicon backing for beam energies ranging from 2 keV down to 250 eV, i.e., beam velocities from  $v/v_0 = 0.6$  down to 0.1. Input parameters reflect the experimental conditions in Ref. [26].

It is seen that in the velocity range covered by Fig. 9, reflection spectra differ qualitatively from quasi single-collision spectra known from Rutherford backscattering.

Consider first the difference between the empty circles, representing

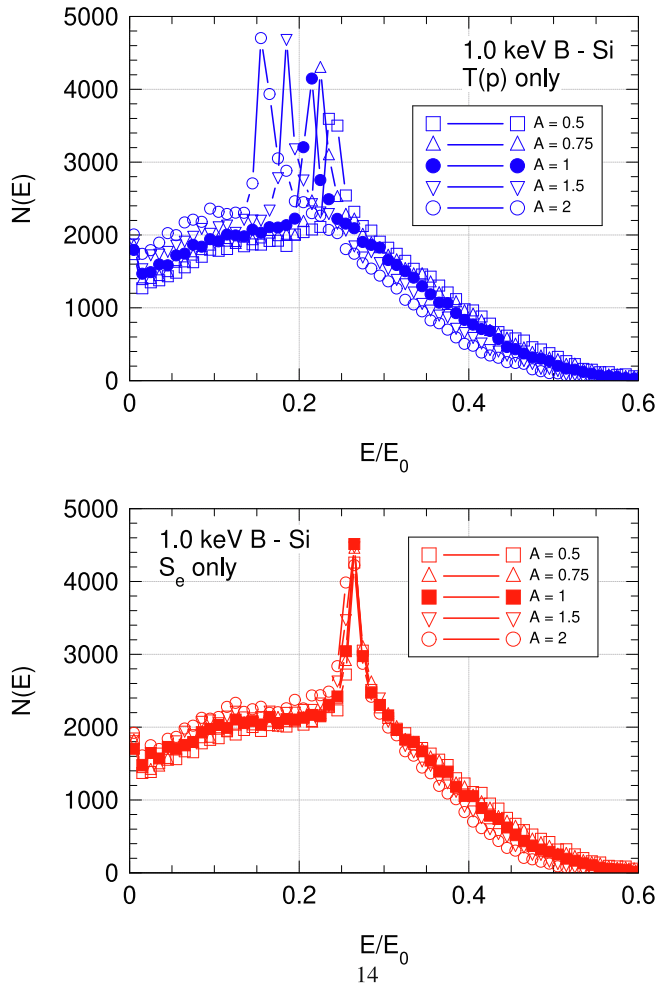


Fig. 7. Same as Fig. 5 for  $E = 1$  keV and five values of the multiplicative factor  $A$  on  $T_e(E, P)$  and  $S_e(E)$ . Top:  $T(p)$ ; bottom:  $S_e$ . Data for  $A \neq 1$  have been normalized to the integral over  $E$  for  $A = 1$ .

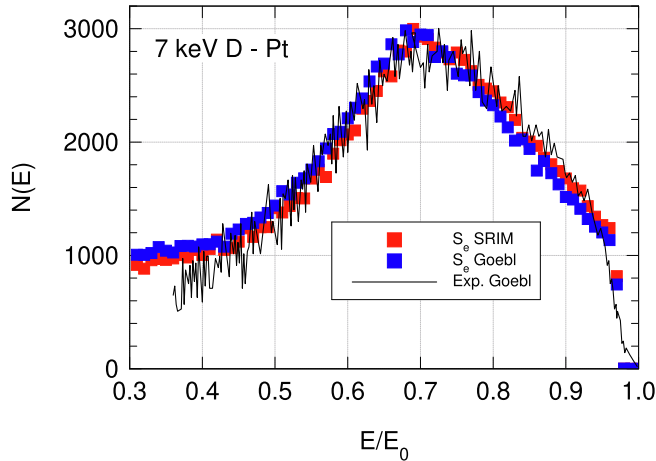


Fig. 8. Reflected energy spectrum for 7 keV D - Pt.  $S_e$  mode width stopping cross sections from SRIM (red filled circles) based on OKSANA and from Goebel et al. [26] (blue filled squares) compared with measurements from [26]. (For interpretation of the references to colour in this figure legend, the reader is referred to the web version of this article.)

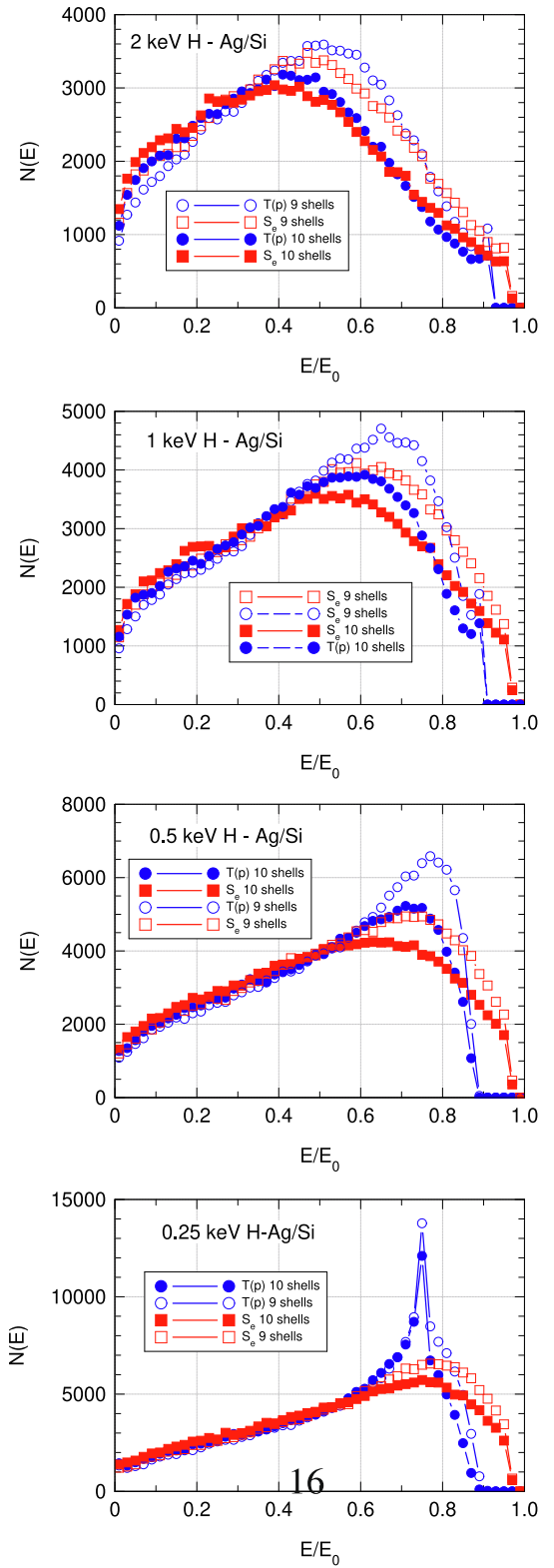
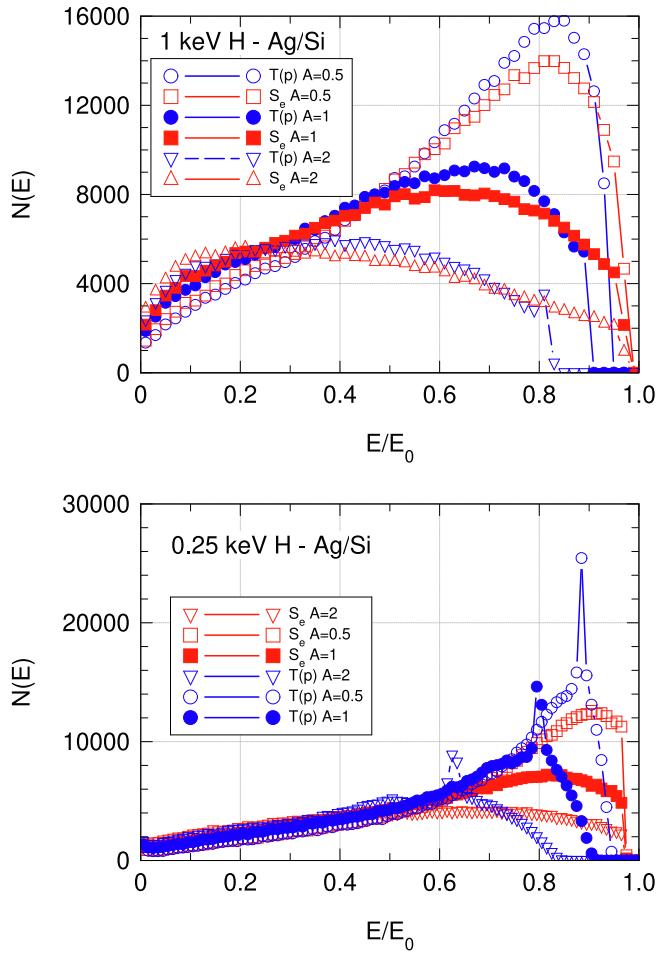


Fig. 9. Energy spectra of protons reflected from a 226 Å silver layer on silicon backing. Primary energy  $E_0$  ranging from 2 keV down to 0.25 keV. Normal incidence. Scattering angle  $155^\circ$ . Computations with PASS output and Thomas-Fermi Molière interaction. Empty symbols: Electronic energy loss to 5s electrons neglected. Filled symbols: Including energy loss from 5s electrons taken as a friction force. 6,000,000 runs.





**Fig. 10.** Dependence of reflection spectra for H-Ag/Si on the absolute magnitude of the stopping cross section, indicated by a multiplicate factor  $A = 2, 1$  and  $0.5$  on  $T(p)$  and  $S_e(E)$ . Top:  $E_0 = 1$  keV. Bottom:  $E = 0.25$  keV. 5s shell of Ag included. No normalization.

$T(p)$  spectra for a 9-shell Ag target, i.e., neglecting 5s electrons, and the empty squares representing the corresponding  $S_e$  spectra. Results are given in absolute values (without normalization) for a fixed number of incident ions (6 000 000). Since measured spectra are in arbitrary units, another scaling could be appropriate, depending on the energy regime analysed.

As to be expected, the maximum of the two curves moves to higher values of  $E/E_0$  as  $E$  decreases, but this shift is more pronounced in the  $S_e$  curves than in the  $T(p)$  curves.

We note that the high-energy cutoff is insensitive to the difference between the  $S_e$  and the  $T(E)$  mode, with the exception of the lowest beam energy, where  $T_e(p = 0)$  is competitive.

More interesting in the present context are spectra including 5s electrons, for which there is no impact-parameter dependence. These spectra are shown as filled circles and squares. The behavior of the maxima as a function of beam energy is qualitatively the same as in the case of 9 shells. The high-energy cutoff is shifted to higher energies and, again, insensitive to beam energy except at 0.25 keV.

Fig. 10 indicates the sensitivity of the reflected-energy spectrum to the magnitude of the electronic stopping cross section for H-Ag/Si at two beam energies. It is seen that in all cases the position of the peaks varies substantially with  $A$ . This implies that even at the lowest energy,  $E_0 = 25$  keV or  $v/v_0 = 1$  spectra are sufficiently sensitive to the stopping

law to allow extraction of valid stopping cross sections.

However, comparison between  $T(p)$  and  $S_e$  data reveals substantial differences in all cases. Again, results are given in absolute values without normalization for a fixed number of incident ions. Thus, basing the analysis of a stopping measurement on the  $S_e$  mode is bound to lead to substantial errors at  $E_0 = 1$  keV. At  $E_0 = 0.25$  keV,  $T(p)$  spectra differ qualitatively from  $S_e$  spectra. Note in particular a significant difference between the peak positions for  $S_e$  and  $T(E)$  mode.

#### 4. Conclusions

- We find that projected ranges computed in the  $S_e$  mode, i.e., describing electronic stopping as a friction force, are in close agreement with the corresponding ranges taking into account the  $p$ -dependence of the electronic energy loss.
- Conversely, energy spectra of reflected ions are sensitive to the impact-parameter dependence. This difference is significantly more pronounced for PASS than for Firsov stopping.
- In the  $S_e$  mode we find good agreement between the present Monte Carlo simulations and those underlying Ref. [28].
- We find pronounced differences in peak position between the  $T(p)$  mode and the  $S_e$  mode. This is important for extracting stopping cross sections by the reflection technique.
- All differences between the two modes increase with decreasing beam energy.
- The difference is less pronounced for conductors than for insulators.

#### Acknowledgement

This work was supported by the Carlsberg foundation.

#### References

- [1] J. Lindhard, M. Scharff, H.E. Schiøtt, *Mat. Fys. Medd. Dan. Vid. Selsk.* 33 (14) (1963) 1.
- [2] J. Lindhard, V. Nielsen, M. Scharff, P.V. Thomsen, *Mat. Fys. Medd. Dan. Vid. Selsk.* 33 (10) (1963) 1.
- [3] J.H. Ormrod, H.E. Duckworth, *Can. J. Phys.* 41 (1963) 1424.
- [4] B. Fastrup, P. Hvelplund, C.A. Sautter, *Mat. Fys. Medd. Dan. Vid. Selsk.* 35 (10) (1966) 1.
- [5] P. Sigmund, A. Schinner, *Nucl. Instrum. Methods B* 410 (2017) 78.
- [6] R. Ishiwari, N. Shiomi, N. Sakamoto, *Phys. Rev. A* 25 (1982) 2524.
- [7] W.N. Lennard, X. Yueyuan, H. Geissel, *Nucl. Instrum. Methods B* 69 (1992) 89.
- [8] A. Schinner, P. Sigmund, *Nucl. Instrum. Methods B* 440 (2019) 41.
- [9] P. Bauer, *Nucl. Instrum. Methods B* 27 (1987) 301.
- [10] W. Eckstein, *Computer Simulation of Ion-solid Interactions*, Springer-Verlag, Berlin, 1991.
- [11] M.T. Robinson, I.M. Torrens, *Phys. Rev. B* 9 (1974) 5008.
- [12] O.S. Oen, M.T. Robinson, *J. Nucl. Mater.* 63 (1976) 210.
- [13] O.B. Firsov, *Zh. Eksp. Teor. Fiz.* 36 (1959) 1517, [Engl. transl. *Sov. Phys. JETP* 9, 1076–1080 (1959)].
- [14] V.I. Shulga, *Appl. Surf. Sci.* 439 (2018) 456.
- [15] P. Sigmund, A. Schinner, *Europ. Phys. J. D* 12 (2000) 425.
- [16] A. Schinner, P. Sigmund, *Europ. Phys. J. D* 56 (2010) 41.
- [17] L.M. Kishinevskii, *Izv. Akad. Nauk SSSR* 26 (1962) 1410, [Engl. transl. *Bull. Acad. Sci. USSR Phys. Ser.* 20, 1433–1438 (1963)].
- [18] N. Bohr, *Philos. Mag.* 25 (1913) 10.
- [19] A. Schinner, P. Sigmund, *Nucl. Instrum. Methods B* 416 (2019) 19.
- [20] P. Sigmund, *Phys. Rev. A* 26 (1982) 2497.
- [21] ICRU, *Stopping of ions heavier than helium*, 73 ICRU Report (Oxford University Press, Oxford, 2005).
- [22] H.H. Mikkelsen, P. Sigmund, *Nucl. Instrum. Methods B* 27 (1987) 266.
- [23] P.L. Grande, G. Schiwietz, *Nucl. Instrum. Methods B* 267 (2009) 859.
- [24] V.I. Shulga, *Radiat. Eff.* 70 (1983) 65.
- [25] J.F. Ziegler, J.P. Biersack, U. Littmark, *The Stopping and Range of Ions in Solids*, 1 The Stopping and Ranges of Ions in Matter, Pergamon, New York, 1985.
- [26] D. Goebel, K. Khalal-Kouache, D. Roth, E. Steinbauer, P. Bauer, *Phys. Rev. A* 88 (2013) 032901.
- [27] S. Naqvi, G. Possnert, D. Primetzhofer, *Nucl. Instrum. Methods B* 371 (2016) 76.
- [28] D. Goebel, D. Roth, P. Bauer, *Phys. Rev. A* 87 (2013).